

# A novel fluorometric detection of $\text{Cu}^{2+}$ based on self-assembled bilayers

Xiang-Ying Sun<sup>a,\*</sup>, Bin Liu<sup>a</sup>, Wen-Ting Weng<sup>a</sup>, Yun-Bao Jiang<sup>b</sup>

<sup>a</sup> College of Material Science and Engineering, Huaqiao University, Quanzhou 362011, China

<sup>b</sup> Department of Chemistry and the MOE Key Laboratory of Analytical Sciences, Xiamen University, Xiamen 361005, China

Received 7 August 2003; received in revised form 27 October 2003; accepted 27 October 2003

## Abstract

Fluorescent reagent sodium 1-naphthylamine diacetate (NADA) was assembled onto gold electrodes via its electrostatic interaction with cysteine (Cys) that was directly assembled on the gold electrode surface. Formation of the self-assembled bilayers was confirmed and primarily characterized by cyclic voltammetry and X-ray photoelectron spectra (XPS). The Cys modification of the gold electrode prevented direct adsorption of NADA onto the gold electrode and hence eliminated fluorescence quenching by gold. Strong fluorescence was observed from the NADA self-assembled bilayers at gold surface and was highly efficiently quenched by  $\text{Cu}^{2+}$  that allowed for an extremely highly sensitive detection of  $\text{Cu}^{2+}$  with a detection limit of 0.2 ppt and quantitative detection range of 0.5–9 ppt. The fluorescence from NADA/Cys/Au can be easily regenerated and therefore the present report showed a reusable method for immobilizing reagent in fabricating fluorescent chemosensors. © 2003 Elsevier B.V. All rights reserved.

**Keywords:** Self-assembled bilayer; Fluorescence sensor;  $\text{Cu}^{2+}$

## 1. Introduction

Much attention has been paid to self-assembled monolayers (SAMs) of thiol or disulfide derivatives on gold electrodes. The SAMs are well-ordered, stable and easy to prepare by a simple one-step adsorption from dilute solutions and have been extensively applied to chemo- and bio-sensing based mostly on electrochemical mechanisms [1–8]. Yet little research has been carried out on the development of SAMs-based fluorescent sensors. This is likely because of the efficient fluorescence quenching on gold electrode surface [9]. Several fluorescent sensors based on SAMs were recently designed by modifying long-chain alkylthiols or mixed SAMs [10,11], in which, however, complicated organic syntheses were involved. Our recent experiments reported in this paper show that indirectly assembling fluorophores onto gold electrodes could efficiently eliminate the fluorescence quenching by gold and therefore fluorescent sensors based on SAMs might be fabricated.

Cysteine is readily available and known to chemisorb on gold electrodes from its dilute solution via the thiol group

[12]. Based on these monolayers we hoped to prepare a fluorophore containing self-assembled bilayers. Cysteine was first assembled onto gold electrode to form a SAM, which was followed by assembling sodium 1-naphthylaminediacetate (NADA) (Scheme 1), a fluorescent amino acid designed for selective and sensitive detection of  $\text{Cu}^{2+}$  [13,14], via its electrostatic interaction with cysteine in the SAM. The formation of the self-assembled bilayers on gold electrode was confirmed and preliminarily characterized by cyclic voltammetry and X-ray photoelectron spectra (XPS). The self-assembled bilayers modified gold electrode was found highly fluorescent and can be used as a fluorescent sensor for  $\text{Cu}^{2+}$  with extremely high sensitivity.

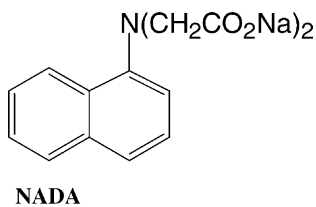
## 2. Experimental

### 2.1. Apparatus

All electrochemical measurements were carried out on a BAS-100B electrochemical analyzer with a conventional three-electrode system using bare or modified Au as working electrode, platinum wire as counter electrode, and Ag/AgCl as reference electrode. The solutions were bubbled with  $\text{N}_2$  for 1 min prior to and during the application of potential.

\* Corresponding author. Tel.: +86-595-2691192; fax: +86-595-2692875.

E-mail address: [liumy@hqu.edu.cn](mailto:liumy@hqu.edu.cn) (X.-Y. Sun).



Scheme 1.

Corrected fluorescence spectra were recorded on a Hitachi F-4500 fluorescence spectrophotometer under excitation at wavelength of 320 nm from a 150W Xe-lamp. The slits for excitation and emission monochromators were both 5 nm. The angle between gold electrode plane and incident excitation light was set at 50° to ensure maximum efficiency for collecting emitting light while avoiding reflection light interference. The angle between gold electrode plane and the emission light was therefore 40°. A 1 cm × 1 cm quartz cell was employed for recording fluorescence spectra.

X-ray photoelectron spectra were obtained with a PHI Quantum 2000 Scanning ESCA Microprobe spectrometer (USA) that focused monochromatic Al K $\alpha$  X-rays onto the sample, and the pass energy was 187.85 eV for wide scans and 46.95 eV for narrow scans, respectively.

## 2.2. Reagents

NADA was synthesized in two steps. Refluxing 1-naphthylamine and chloroacetic acid in aqueous NaOH solution afforded 1-(naphthyl)aminoacetic acid (NAA) [15], which was purified by repeated recrystallizations from ethanol.  $^1\text{H}$  NMR (DMSO- $d_6$ , TMS, 500 MHz):  $\delta$  (ppm) 12.50 (CO $_2$ H), 8.122–8.106 (1H, d), 7.779–7.762 (1H, d), 7.449–7.421 (2H, m), 7.279–7.248 (1H, t), 7.146–7.130 (1H, d), 6.352–6.337 (1H, d), 3.979 (2H, s), 3.348 (s, NH). Further reaction of NAA with chloroacetic acid led to NADA that was purified by silica-gel column chromatography using absolute ethanol as eluent.  $^1\text{H}$  NMR (D $_2$ O, TMS, 500 MHz):  $\delta$  (ppm) 8.259–8.244 (1H, d), 7.918–7.902 (1H, d), 7.573–7.535 (3H, m), 7.439–7.423 (1H, t), 7.081–7.067 (1H, d), 3.896 (4H, s). The fluorescence parameters of NAA and NADA have been reported elsewhere [13,14,16,17].

All chemicals were of analytical grade or above. Aqueous solutions were prepared using water purified by a Millipore Milli-Q system (18 M $\Omega$  cm).

## 2.3. Electrode preparation

The gold electrodes were first polished, using 1.0, 0.3 and 0.05  $\mu\text{m}$  alumina slurries, respectively, on microcloth pads to a mirror-like finish. After removal of the trace amount of alumina from the electrode surface, it was rinsed in water and briefly cleaned in an ultrasonic bath, and finally cleaned by cycling between  $-0.5$  and  $+1.5$  V (versus Ag/AgCl) in 1 mol l $^{-1}$  H $_2$ SO $_4$  at a scan rate of 100 mV s $^{-1}$ .

The electrodes were thoroughly rinsed with ultra-pure water (Milli-Q) before thiol chemisorption.

Adsorption of cysteine was carried out by dipping cleaned gold electrodes in 0.01 mol l $^{-1}$  cysteine solution at pH 5.7 for 3 h, followed by rinsing thoroughly in ultra-pure water and drying with N $_2$ . Under these conditions cysteine was adsorbed on the gold electrode in the form of  $-\text{SCH}_2\text{CHNH}_3^+\text{CO}_2\text{H}$  [18].

NADA/Cys/Au electrode was fabricated by immersing the cysteine modified gold electrode in 0.5 mol l $^{-1}$  HCl for 10 min, and then into 0.01 mol l $^{-1}$  NADA solution of pH 5–6 for 1 h. NADA was electrostatically bound to cysteine modified gold electrodes and the fluorescent self-assembled bilayer electrodes were obtained.

## 3. Results and discussion

### 3.1. Optimal conditions for preparation of NADA/Cys/Au electrodes

The blank Au electrode was immersed in cysteine solutions of varied concentration ranging from 0.001 to 0.1 mol l $^{-1}$  for different durations. The optimal conditions for adsorption of cysteine onto gold surface are dipping cleaned gold electrodes in 0.01 mol l $^{-1}$  cysteine solution at pH 5.7 for 3 h. Under these conditions a coverage of cysteine on gold surface of  $4.3 \times 10^{-11}$  mol cm $^{-2}$  was determined from the area of the reduction peak at  $-0.768$  V (versus Ag/AgCl) in the CV of cysteine recorded in deoxygenated 0.5 mol l $^{-1}$  KOH solution.

NADA solutions of varied pH were chosen to adjust the charge states of NADA molecule in order to enhance its electrostatic interaction with cysteine that has already been assembled on the gold electrode surface. Experiments showed that a stable fluorescent self-assembled bilayer on gold electrode (NADA/Cys/Au) was formed by dipping Cys/Au electrode in 0.01 mol l $^{-1}$  NADA solution of pH 5–6 for 1 h.

### 3.2. Electrochemical characterization of self-assembled monolayer and bilayer

The assembling of cysteine and NADA was first examined by cyclic voltammetry (CV). Fig. 1 shows the cyclic voltammograms (CVs) of blank Au electrode and cysteine assembled Au electrode (Cys/Au) in 0.05 mol l $^{-1}$  Na $_2$ B $_4$ O $_7$ ·10H $_2$ O–NaOH–CH $_3$ CHO solution of pH 9.6. Compared with the CV of blank Au electrode, that of the Cys/Au electrode showed an irreversible oxidation peak at  $+0.93$  V (versus Ag/AgCl). The peak current increased with increasing cysteine concentration, suggesting that cysteine was assembled on the gold electrode.

Fig. 2 shows the CVs of NADA/Cys/Au and Cys/Au working electrodes in  $5 \times 10^{-4}$  mol l $^{-1}$  KNO $_3$  solution containing 3 ppm Cu $^{2+}$ . It was noted that reduction/oxidation of Cu $^{2+}$  at the NADA/Cys/Au electrode became much

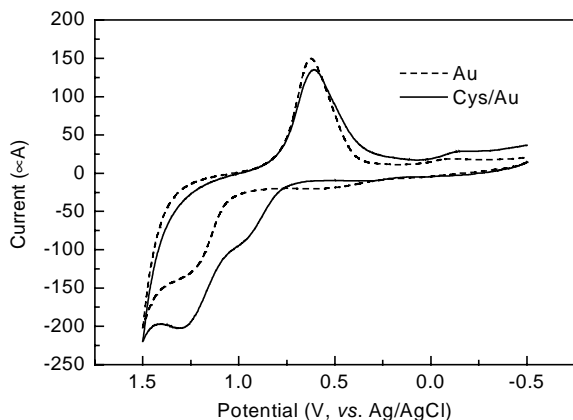


Fig. 1. Cyclic voltammograms of blank Au electrode and Cys/Au electrode in  $0.05 \text{ mol l}^{-1}$  of  $\text{Na}_2\text{B}_4\text{O}_7 \cdot 10\text{H}_2\text{O}$ – $\text{NaOH}$ – $\text{CH}_3\text{CHO}$  solution of pH 9.6. Scan rate was  $100 \text{ mV s}^{-1}$ .

more irreversible compared with that at the Cys/Au electrode, which suggested that NADA was assembled onto the Cys/Au electrode surface and inhibited the electrochemistry reaction of  $\text{Cu}^{2+}$ .

### 3.3. XPS experiments on self-assembled monolayer and bilayer

Figs. 3 and 4 show the X-ray photoelectron spectra of NADA/Cys/Au and Cys/Au electrodes, respectively. The observed Au 4f binding energy of 84.3 eV in NADA/Cys/Au and of 84.1 eV in Cys/Au suggested that the substrate was unaffected during NADA assembling onto the surface of gold. Compared with those in the XPS of Cys/Au electrode, the intensities of O 1s and C 1s peaks of NADA/Cys/Au increased substantially. The nitrogen binding energies were found as 399.4 eV and 400.6 eV, which are attributed to  $-\text{N}$  in NADA and  $-\text{NH}_3^+$  in cysteine, respectively. These XPS data further supported that NADA and cysteine were assembled onto the gold electrode and were consistent with the

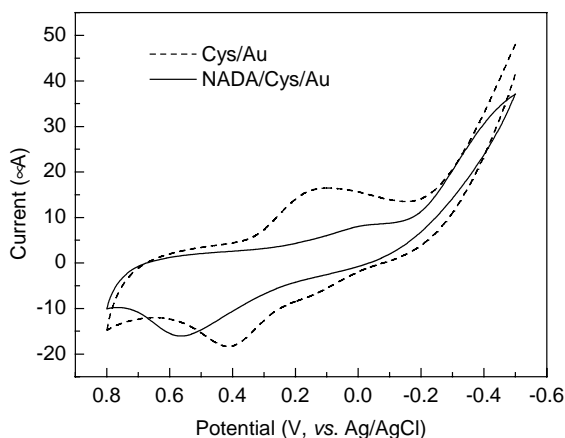


Fig. 2. Cyclic voltammograms of Cys/Au and NADA/Cys/Au electrodes in  $5 \times 10^{-4} \text{ mol l}^{-1}$   $\text{KNO}_3$  solution containing 3 ppm  $\text{Cu}^{2+}$ . Scan rate was  $100 \text{ mV s}^{-1}$ .

results of electrochemical data and fluorimetric studies reported later. The fact that a new peak appearing at 932.7 eV after exposing to  $\text{Cu}^{2+}$  solution of the NADA/Cys/Au electrode (Fig. 5) suggested that  $\text{Cu}^{2+}$  coordinated onto the surface of NADA/Cys/Au electrode.

### 3.4. Fluorescence properties of NADA/Cys/Au electrode

Fig. 6a shows the surface fluorescence spectra of NADA/Cys/Au, Cys/Au, NADA/Au and blank Au electrodes under the excitation of 320 nm light from a 150 W Xe-lamp. It was found that the NADA/Cys/Au electrode emitted NADA-characteristic fluorescence, further confirming that NADA was assembled on Au electrode surface. The fact that NADA/Au electrode did not show any fluorescence emission while strong fluorescence emission was detected from NADA/Cys/Au electrode indicated that cysteine modification in NADA/Cys/Au electrode prevented the direct contact of NADA with the gold electrode surface and hence the interactions between fluorescing molecules and the free electrons in the metal that resulted in rapid transfer of energy and relaxation responsible for gold-surface fluorescence quenching. The fluorescence emission of NADA/Cys/Au electrode peaked at 403 nm was blue-shifted by 35 nm from that of NADA bulk solution at 438 nm (Fig. 6b). This is probably due to the varied microenvironment for NADA molecules in the self-assembled bilayer on gold electrode from that in bulk solution [19] so that NADA existed in a more hydrophobic environment in the bilayers.

NADA/Cys/Au electrode thus prepared was found highly stable that practically no fluorescence could be detected from aqueous phase after 1 day of immersing the self-assembled bilayer electrodes in it.

### 3.5. Fluorescent sensor for $\text{Cu}^{2+}$

NADA was previously designed as a solution-phase fluorescent sensor for  $\text{Cu}^{2+}$  based on fluorescence quenching by  $\text{Cu}^{2+}$  [14]. The quenching observed in 30% ethanol aqueous solution was found to obey Stern–Volmer theory described in Eq. (1), [14]:

$$\frac{I_0}{I} = 1 + K_{\text{SV}}[Q] \quad (1)$$

in which  $I_0$  and  $I$  represent fluorescence intensities in the absence and presence of quencher of concentration  $[Q]$ , respectively. Similar experiments were repeated in aqueous solutions without ethanol and a quenching constant  $K_{\text{SV}}$  of  $\text{Cu}^{2+}$  to NADA solution fluorescence  $4.2 \times 10^4 \text{ mol l}^{-1}$  was found to be higher than those of other metal ions of similar electronic structure such as  $\text{Co}^{2+}$ ,  $\text{Ni}^{2+}$  and  $\text{Zn}^{2+}$ . In bulk aqueous solution without ethanol NADA was thus shown to be a sensitive reagent for detection of  $\text{Cu}^{2+}$ .

Fluorescence of NADA/Cys/Au electrode was found quenched by  $\text{Cu}^{2+}$  in the aqueous solution, Fig. 7. It was observed from Fig. 7 that the intensity of fluorescence

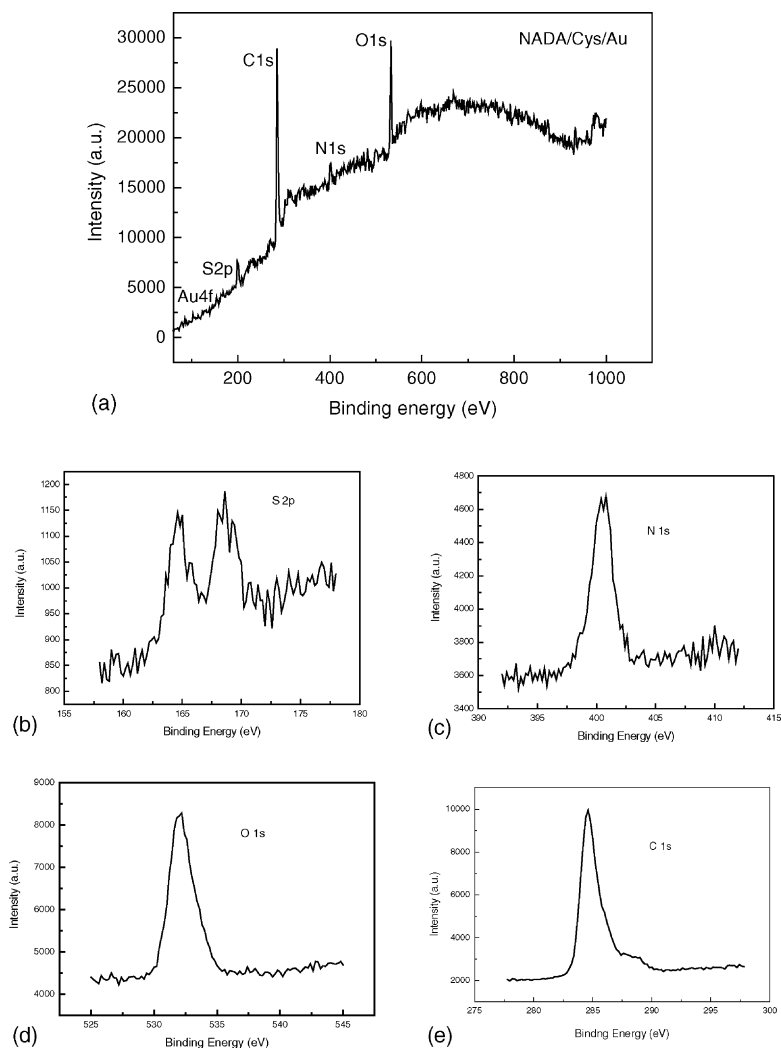


Fig. 3. XPS of NADA/Cys/Au electrode. (a) Wide view, (b) S 2p spectrum, (c) N 1s spectrum, (d) O 1s spectrum, and (e) C 1s spectrum.

emission peaked at 403 nm decreased with increasing  $\text{Cu}^{2+}$  concentration in the Stern–Volmer manner (Fig. 8). A quenching constant  $K_{SV}$  of  $4.1 \times 10^9 \text{ mol}^{-1}$  for  $\text{Cu}^{2+}$  to the NADA/Cys/Au was obtained (data from four NADA/Cys/Au

electrode's relative standard deviation = 0.3), which is five orders of magnitude higher than that obtained for solution phase fluorescence quenching. Compared with NADA solution-phase measurement, NADA/Cys/Au electrode's

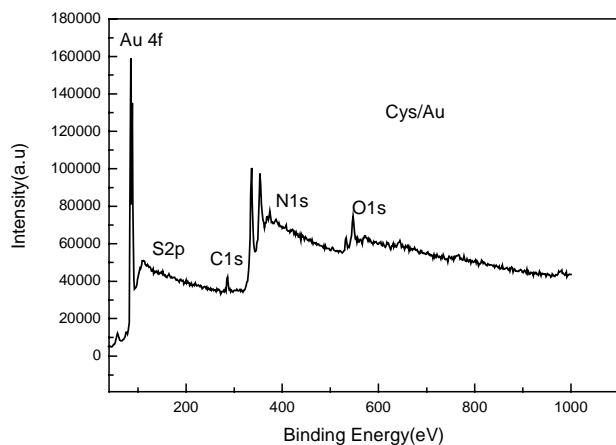


Fig. 4. XPS of Cys/Au electrode.

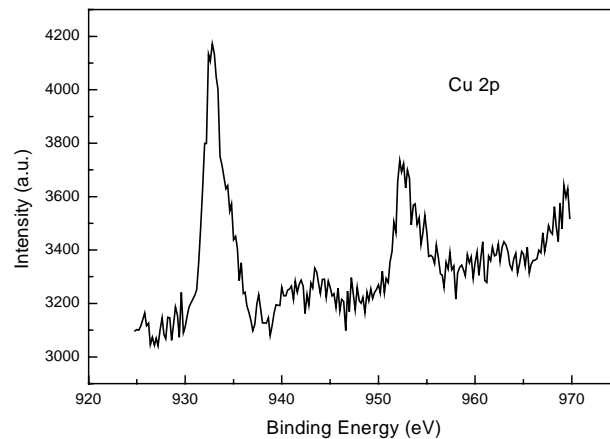


Fig. 5. Cu 2p spectrum of NADA/Cys/Au electrode after immersion in  $\text{Cu}^{2+}$  solution.

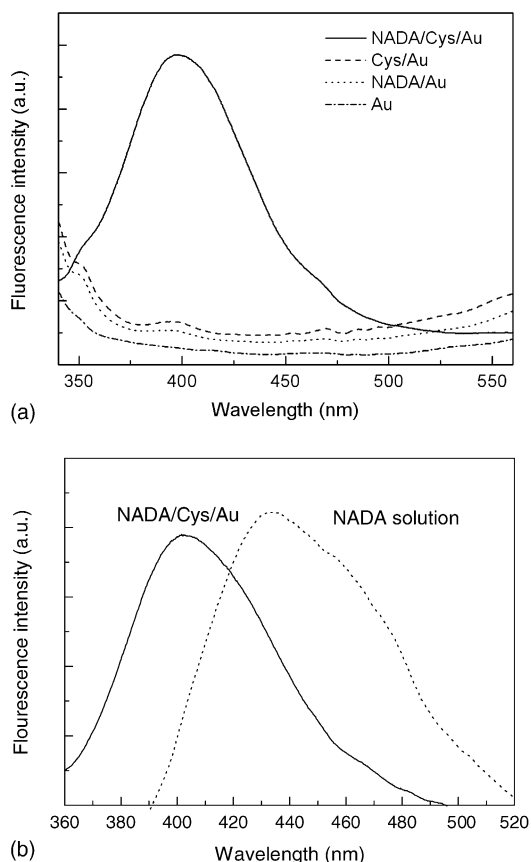


Fig. 6. (a) Surface fluorescence spectra of NADA/Cys/Au, Cys/Au, NADA/Au, and blank Au electrodes and (b) fluorescence spectra of NADA/Cys/Au electrode and NADA solution of pH 6. The “emission signals” shown in (a) for Cys/Au, NADA/Au, and Au electrodes are due to scattering light.

sensitivity for fluorimetric detection of  $\text{Cu}^{2+}$  is substantially increased, as clearly seen in Fig. 8. Linear range for quantitative detection of  $\text{Cu}^{2+}$  was 0.5–9 ppt with a detection limit ( $3\text{S.D.}/K$ ) of 0.2 ppt which is five orders of magnitude lower than that of the bulk solution-phase

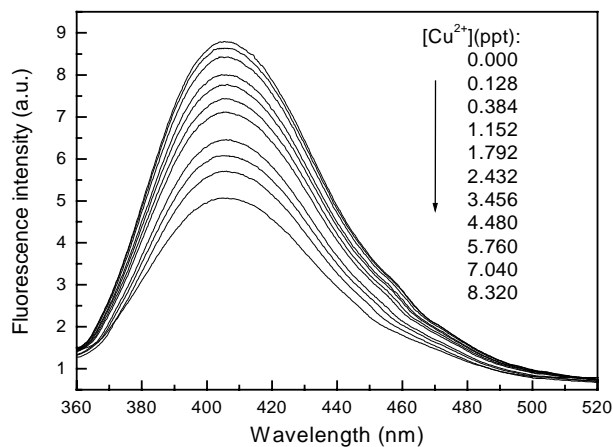


Fig. 7. Fluorescence spectra of NADA/Cys/Au electrode in aqueous solutions containing  $\text{Cu}^{2+}$  of varied concentration.

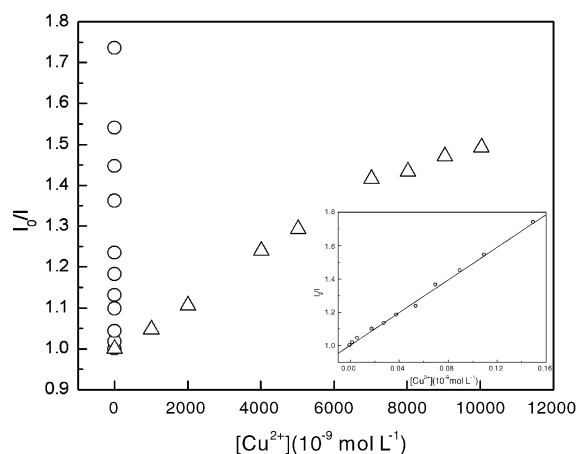


Fig. 8. Stern–Volmer plots of NADA/Cys/Au electrode and NADA solution fluorescence quenching by  $\text{Cu}^{2+}$ . (○) NADA/Cys/Au electrode in aqueous solution, (△) NADA in bulk aqueous solution. Inset shows expanded Stern–Volmer plot for the NADA/Cys/Au electrode fluorescence quenching.

detection limit of 54 ppb. It is thus shown that with the fluorophore containing self-assembled bilayer on gold surface the analysis sensitivity was greatly enhanced compared to that of the corresponding solution-phase analysis, although at the moment we are still unable to figure out the enhancing mechanism. Our preliminary experiments showed that the presence of less than 200 equivalents of  $\text{Pb}^{2+}$ , 100 equivalents of  $\text{Zn}^{2+}$ , 300 equivalents of  $\text{Cd}^{2+}$ , 20 equivalents of  $\text{Ni}^{2+}$ , and 10 equivalents of  $\text{Co}^{2+}$ , respectively, did not lead to interference of the fluorimetric detection of  $\text{Cu}^{2+}$  by 10% change in the emission intensity. Common ions such as  $\text{K}^+$ ,  $\text{Na}^+$ ,  $\text{Cl}^-$ , and  $\text{NO}_3^-$  had no influence on the assays. The method was successfully applied to the determination of  $\text{Cu}^{2+}$  in water samples with satisfactory recoveries of 91.4, 91.3 and 93.4% for tap, lake and ground water samples, respectively.

### 3.6. Fluorescence reversibility

Reversibility is an important parameter of a sensor. It is desirable that, after the analysis, the sensor-analyte complexation could be readily reversed. In this process, the analyte ( $\text{Cu}^{2+}$  herein) was released from the sensor membrane, so that the sensor was restored to its original form and ready for the next measurement. We examined the reversibility of the NADA/Cys/Au electrode by following its fluorescence variations. The NADA/Cys/Au electrode was put in  $\text{Cu}^{2+}$  solution, the fluorescence intensity decreased with the immersion time. When the electrode was re-put in  $0.1\text{ mol l}^{-1}$  HCl solution for 30 min and then in ultra-pure water, the fluorescence was efficiently regenerated to more than 97% of its original intensity. Therefore, an excellent reversibility was observed with the fluorescence of this NADA/Cys/Au sensor.

#### 4. Conclusions

By the mediation of cysteine, NADA was successfully assembled onto the gold electrode via its electrostatic interaction with cysteine that was directly assembled on the gold electrode. The fluorescent NADA/Cys/Au electrode thus prepared was found highly fluorescent and successfully applied to fluorimetric detection of copper ion with good stability and extremely high sensitivity. The fluorescent electrode could be easily recovered after measurements and thereby the self-assembling method reported here represents a new way of immobilizing fluorescent reagent for a sensor in a reusable manner. The results should also provide a hint of the high potentials of self-assembled bilayer modified electrodes in fluorescent sensing since the possible electrochemical perturbations may exert additional influences for improving the sensing performance.

#### Acknowledgements

This work was supported by the Foundation of Overseas-Chinese Affairs Office of the State Council of China (grant No. 03QZR12), National Natural Science Foundation of China (grant No. 20175020) and VolkswagenStiftung (grant No. I/77 072).

#### References

- [1] A. Ulman, J.F. Kang, Y. Shnidman, S. Liao, R. Jordan, G.Y. Choi, J. Zaccaro, A.S. Myerson, M. Rafailovich, J. Sokolov, C. Fleischer, *Rev. Mol. Biotech.* 74 (2000) 175.
- [2] H. Nagatani, D.J. Fermin, H.H. Girault, *J. Phys. Chem. B* 105 (2001) 9463.
- [3] L.B. Israel, N.N. Kariuki, L. Han, M. Maye, J. Luo, C.J. Zhong, *J. Electroanal. Chem.* 517 (2001) 69.
- [4] J.L. Tan, J. Tien, C.S. Chen, *Langmuir* 18 (2002) 519.
- [5] N.K. Chaki, K. Vijayamohan, *Biosens. Bioelectron.* 17 (2002) 1.
- [6] J.J. Gooding, D.B. Hibbert, *Trends Anal. Chem.* 18 (1999) 525.
- [7] W. Yang, D. Jaramillo, J.J. Gooding, D.B. Hibbert, R. Zhang, G.D. Willett, K.J. Fisher, *Chem. Commun.* (2001) 1982.
- [8] J.M. Pope, D.A. Buttry, *J. Electroanal. Chem.* 498 (2001) 75.
- [9] A. Ishida, T. Majima, *Analyst* 125 (2000) 535.
- [10] K. Motesarei, D.C. Myles, *J. Am. Chem. Soc.* 120 (1998) 7328.
- [11] V.H. Perez-Luna, M.J. O'Brien, K.A. Opperman, P.D. Hampton, G.P. Lopez, L.A. Klumb, P.S. Stayton, *J. Am. Chem. Soc.* 121 (1999) 6469.
- [12] D.W.M. Arrigan, L.L. Bihan, *Analyst* 124 (1999) 1645.
- [13] X.-Y. Sun, Y.-B. Jiang, *Anal. Sci* 17 (Suppl.) (2001) 1461.
- [14] X.-Y. Sun, B. Liu, J.-R. Xu, *Chin. J. Anal. Lab.* 21 (2002) 60.
- [15] Y.T. Chen, S.C. Wang, L.L. Zhou, *Acta Chimica Sinica* 25 (1959) 377.
- [16] L.-H. Ma, Z.-C. Wen, X.-Y. Sun, Y.-B. Jiang, *Chem. J. Chin. Univ.* 21 (2000) 1377.
- [17] X.-Y. Sun, Z.-C. Wen, Y.-B. Jiang, *Chin. J. Chem.* 21 (2003) 1335.
- [18] A.G. Brolo, P. Germain, G. Hager, *J. Phys. Chem. B* 106 (2002) 5982.
- [19] R.R. Naujok, R.V. Duevel, R.M. Corn, *Langmuir* 9 (1993) 1771.